

with respect to the molecular reference frame. This assignment resulted by requiring that  $\sigma_{11}$  and  $\sigma_{22}$ , with eigenvalues differing by only 20 ppm compared to a total anisotropy of 197 ppm, have similar orthogonal shielding environments. The second criterion required  $\sigma_{33}$ , the least shielded element, to be oriented normal to the water-oxygen plane. In this case compliance with one criterion guaranteed the second. The tensor element,  $\sigma_{11}$  is coincidental with  $c$  (the  $C_2$  axis) and hence bisects the O(4)-Cd-O(4') angle (see Table V). The two shielded elements lie in the water-oxygen plane making angles of 88 and 84°,  $\sigma_{11}$  and  $\sigma_{22}$ , respectively, with the normal to the BLP defined by Cd and the four water oxygens. Further,  $\sigma_{11}$  is oriented 76 and 78° from the Cd-O(2) and Cd-O(2') internuclear vectors, respectively, and 104 and 110° from the Cd-O(1) and Cd-O(1') vectors, respectively. This corresponds to  $\sigma_{11}$ -best-line angles of 87 and 88°, respectively. Again, the perpendicular orientation of the most shielded element with the longest Cd-O bond should be noted.  $\sigma_{22}$  has a comparable orientation relative to the Cd-O<sub>2</sub>NO<sup>-</sup> bonds. However, as might be anticipated, the  $\sigma_{22}$  BLL angles are less (63 and 78° for lines corresponding to O(1)-Cd-O(1') and O(2)-Cd-O(2') than the corresponding  $\sigma_{11}$  angles. Finally,  $\sigma_{33}$ , the least shielded element, makes an acute angle of 83° with the BLP defined by Cd-O(3), O(3'), O(4), and O(4').

The alternative assignment, which is easily visualized in Figure 5, corresponds to reflection of the shielding tensor in the  $b,c$  plane. This assignment results in  $\sigma_{11}$  and  $\sigma_{33}$ , the most shielded and deshielded elements, having similar orthogonal environments. We contend that this is an unreasonable configuration.

### Conclusion

The orientation of three distinct <sup>113</sup>Cd shielding tensors relative to the corresponding oxo-cadmium molecular reference frames has been determined. The local Cd site symmetry has been observed to dominate the orientation of the tensor. The orientation of the shielding tensor corresponding to the special position in

3CdSO<sub>4</sub>·8H<sub>2</sub>O was unambiguously determined by NMR and crystallographic data. The shielding tensor-molecular reference frame orientation for cadmium sulfate general position and cadmium nitrate (Cd(NO<sub>3</sub>)<sub>2</sub>·4H<sub>2</sub>O) required assumptions. Three observations correlating shielding tensor element orientation with molecular features were made and are reiterated. First, shielding tensor elements of comparable magnitude have similar molecular environments normal to the elements. Second, the least shielded tensor elements are aligned nearly perpendicular to planes containing water oxygen. Third, the more shielded tensor elements are oriented perpendicular to the longer Cd-O bonds. Clearly, additional single-crystal NMR data for oxo-cadmium complexes are required to determine whether these orientational features are general or unique to the compounds investigated in this work.

Finally, correlations between bond-length dispersion and shielding anisotropy have been suggested.<sup>11d</sup> At this point, our data on <sup>113</sup>Cd shielding tensors, do not indicate a direct correlation between bond-length variation and the magnitude of the shielding anisotropy. Bond-length dispersion, local site symmetry, and ligand type are all contributory structural parameters in determining the value of  $\Delta\sigma$ .

**Acknowledgment.** The authors thank Dr. J. W. Richardson and Professor R. A. Jacobsen for kindly supplying the crystal structure data for 3CdSO<sub>4</sub>·8H<sub>2</sub>O. Further, we thank the crystallography group at U.S.C., Professor E. L. Amma and Drs. E. H. Griffith, R. C. Paslay, and N. G. Charles, for the helpful discussions during the course of this work and for supplying access to the necessary diffraction equipment. The use of the facilities at the University of South Carolina NMR Center, funded by the National Science Foundation (CHE 78-18723), is acknowledged. Finally, we acknowledge the National Institutes of Health (GM 26295) for partial support of this research.

**Registry No.** <sup>113</sup>Cd, 14336-66-4; Cd(NO<sub>3</sub>)<sub>2</sub>·4H<sub>2</sub>O, 10022-68-1; 3CdSO<sub>4</sub>·8H<sub>2</sub>O, 7790-84-3.

## The Interaction of Lanthanide Shift Reagents with Cationic Sites: A <sup>1</sup>H and <sup>13</sup>C NMR Study of the Solution Geometry of Nicotine *N*-Methiodide

Ronald L. Bassfield

Contribution from the Philip Morris U.S.A. Research Center, Richmond, Virginia 23261.  
Received August 20, 1982

**Abstract:** The use of lanthanide shift reagents as proton and carbon-13 NMR shift and relaxation probes has enabled the determination of the solution geometry of the nicotine *N*-methiodide complex. A series of experiments were performed to illustrate the applicability of induced shift and  $T_1$  relaxation data derived from the interaction between Ln(fod)<sub>3</sub> and a quaternary ammonium salt. The results indicate that the lanthanide/anion moiety complexes with quaternary salts via the positively charged center and adheres principally to the pseudocontact model.

We previously reported the interaction of lanthanide shift reagents (LSR) with bifunctional ammonium salts containing both a positive quaternary nitrogen and a neutral amine nitrogen.<sup>1</sup> The results of that study revealed that the LSR complexes preferentially with the negative counterion rather than with the lone pair of electrons of the amine nitrogen. It was suggested that the observed paramagnetic shifts in the cationic moiety resulted from the tight ion pairing of the LSR-anion adduct and the cationic

species. The ion pairing phenomenon is enhanced by the use of a nonpolar solvent such as chloroform-*d*. Although ion pairing of LSR-anion complexes with positively charged centers has been reported,<sup>2-9</sup> to our knowledge no detailed structural analysis has

(2) K. B. Lipkowitz, T. Chevalier, B. P. Mundy, and J. J. Theodore, *Tetrahedron Lett.*, **21**, 1297 (1980).

(3) F. Lefevre, C. Rabiller, A. Mannshreck, and G. J. Martin, *J. Chem. Soc., Chem. Commun.*, 942, (1979).

(4) Alexandru T. Balaban, *Tetrahedron Lett.*, **50**, 5055 (1978).

(5) G. Montavdo, *Tetrahedron Lett.*, **21**, 1841 (1974).

(1) J. I. Seeman and R. L. Bassfield, *J. Org. Chem.*, **42**, 2337 (1977).

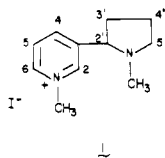
Table I. Experimental and Calculated Shifts with the Corresponding  $F_n$  and  $G_n$  Factors

proton obsd	Pr		Eu		Ho		Er		Yb		std dev	$F_n$	$G_n$
	$\nu_{\text{obsd}}$	$\nu_{\text{calcd}}$	$\nu_{\text{obsd}}$	$\nu_{\text{calcd}}$	$\nu_{\text{obsd}}$	$\nu_{\text{calcd}}$	$\nu_{\text{obsd}}$	$\nu_{\text{calcd}}$	$\nu_{\text{obsd}}$	$\nu_{\text{calcd}}$			
<i>N</i> -CH <sub>3</sub>	-1.22	-1.97	1.4	1.4	-7.4	-7.1	8.3	7.5	3.7	4.95	1.16	-0.02 ± 0.06	0.21 ± 0.02
5'	-0.45	-0.99	1.2	1.29	-5.0	-4.8	6.1	5.6	3.0	3.8	0.82	-0.008 ± 0.04	0.15 ± 0.02
2'	-1.3	-2.38	2.4	2.13	-10.0	-9.6	11.4	10.3	5.0	6.95	1.76	-0.024 ± 0.09	0.28 ± 0.03
<i>N</i> '-CH <sub>3</sub>	-13.1	-22.4	9.6	9.52	-66.3	-62.9	72.4	63.1	23.4	38.6	14.44	-0.37 ± 0.74	1.78 ± 0.27
5	-7.5	-14.1	5.34	5.79	-41.6	-39.4	45.9	39.2	13.4	23.9	10.17	-0.23 ± 0.52	1.12 ± 0.19
4	-2.8	-4.2	2.42	2.39	-15.7	-15.1	15.9	14.5	7.4	9.7	2.11	-0.24 ± 0.11	0.41 ± 0.04
2	-6.6	-8.9	3.22	2.33	-26.8	-25.7	24.5	22.3	9.6	13.8	3.88	-0.08 ± 0.02	0.67 ± 0.07
6	-23.4	-36.6	15.9	12.3	-109.3	-103.6	109.3	96.5	35.7	59.3	21.74	-0.48 ± 0.14	2.83 ± 0.40

been reported utilizing the information gained from the complexation of LSR's with these types of substrates.

In general the observed paramagnetic shifts attributed to LSR's are a combination of contact, pseudocontact or dipolar, and complex formation terms. With lanthanide induced shift (LIS) studies of ion paired complexes, it is postulated that there is no direct coordination between the LSR and a specific donor nucleus of the substrate molecule. This assumption suggests that the observed shifts are derived from purely dipolar, "through space" interactions, thus yielding valuable information about the time-averaged solution geometry of the substrate. However, unlike the classical LSR/substrate complexes, there are no compelling arguments to support any specific geometry for the orientation of the LSR/anion adduct with respect to the positive center of substrate. As a result, the orientation of the principal magnetic axis of the shift reagent is undefined. This fact introduces additional unknowns into the structural analysis.

For the purpose of this study, the interactions of nicotine *N*-methiodide (1) and several LSR's and Gd(fod)<sub>3</sub> (a lanthanide relaxation reagent, LRR) were investigated. Initially the hypothesis of purely dipolar interactions was tested by application of a detailed analysis to determine the best fit of chemical shift data to the geometry of the LSR/substrate complex. If dipolar interactions are demonstrated, then LSR and LRR data may be used together to treat the conformational analysis more simply.



Ultimately, the scope of this study is seen as an attempt at assessing the feasibility of LSR's and LRR's as conformational probes for this class of organic compounds.

### Experimental Section

Nicotine *N*-methiodide was prepared by following the published procedure of Seeman and Whidby.<sup>10</sup>

The LSR (type Ln(fod)<sub>3</sub>: where Ln = Er, Eu, Ho, Pr, and Yb) and Gd(fod)<sub>3</sub> used in this study were purchased from the Norell Chemical Company, Inc. and used without further purification. The diamagnetic La(fod)<sub>3</sub> was prepared according to the literature procedure of Sievers,<sup>11</sup> i.e., adding a slightly basic fod (PCR Inc.) solution to an alcoholic solution of La(NO<sub>3</sub>)<sub>3</sub>·5H<sub>2</sub>O (Alfa Products). The resulting product was recrystallized from methylene chloride and vacuum dried at 80 °C for several days in order to obtain the anhydrous product. The shift reagents were stored in a vacuum desiccator over P<sub>2</sub>O<sub>5</sub>. Sample preparations were carried out in a glovebag under dry nitrogen.

<sup>1</sup>H (80.0 MHz) and <sup>13</sup>C (20.1 MHz) NMR spectra were obtained on a Bruker WP-80 FT spectrometer operating at ambient probe tempera-

ture (303 ± 1 K). Chemical shifts are referenced downfield from Me<sub>4</sub>Si.

LIS data were obtained by the incremental addition of a stock solution of LSR to an NMR tube containing a CDCl<sub>3</sub> solution of the substrate. Molar ratios [LSR]/[substrate] ranged from 0.01 to 0.1 for the paramagnetic ions and 0.1 to 0.7 for La(fod)<sub>3</sub>. Gd(fod)<sub>3</sub>/substrate molar ratios were in the range of 10<sup>-3</sup> in order to avoid severe line broadening.

The paramagnetic shifts corresponding to 1:1 complexes were extrapolated from the slopes of plots of the molar ratio vs. the induced shifts. In all cases, the correlation coefficients of the calculated lines were better than 0.99 except in instances where the total shift difference was <0.1 ppm.

<sup>1</sup>H and <sup>13</sup>C T<sub>1</sub> measurements were made by using the 180°-τ-90° inversion-recovery pulse sequence and the T<sub>1</sub> values were calculated by using a three-parameter exponential fit program.<sup>12</sup> The reported proton 1/T<sub>1</sub> values represent the slope of a plot of the molar ratio vs. the T<sub>1</sub> value. Each data set contained no less than three molar ratio concentrations with at least ten incremental τ values.

The computer analyses were done on a Xerox Sigma-IX computer.

### Results and Discussion

**LIS and Relaxation Studies.** The LIS data were consistent in magnitude and sign throughout the series of lanthanide ions investigated. In all the LIS experiments, protons in proximity to the positive charge displayed the greatest perturbation. Listed in the order of decreasing magnitude, the induced shifts were as follows (see Table I): 6 > *N*-CH<sub>3</sub> > 5 > 2 > 4 > 2' > *N*'-CH<sub>3</sub> > 5'. This ordering of the paramagnetic shifts suggests, at least qualitatively, that the lanthanide complexed adduct is in the vicinity of the pyridyl nitrogen and therefore away from the nitrogen lone pair electrons of the pyrrolidine ring.

The utility of LSR's is derived from the anisotropic dipolar shielding field which surrounds the metal and its directly bound ligand. When the LSR undergoes complexation, the magnitude of the shifts of nuclei within the substrate is dependent upon the location of that nucleus within this shielding field. Since the spatial shape of this field can be defined with well-known equations, it is therefore possible to calculate a solution geometry of that substrate. This procedure is based on the relationship between the dipolar shifts, Δ*v*<sub>pc</sub>, and the position of a given nucleus relative to the lanthanide ion as shown in eq 1,<sup>13</sup> where *r*<sub>*i*</sub> is the distance

$$\Delta v_{pc} = \frac{K_1(1 - 3 \cos^2 \theta_i)}{r_i^3} + \frac{K_2(\sin^2 \theta_i \cos 2\phi_i)}{r_i^3} \quad (1)$$

vector between the metal ion and nucleus *i*, and θ<sub>*i*</sub> and φ<sub>*i*</sub> are the angles formed by *r*<sub>*i*</sub> and the *Z* and *X* axis, respectively. *K*<sub>1</sub> and *K*<sub>2</sub> are constants which depend on the particular lanthanide ion under investigation. If the anisotropic distribution of the paramagnetic center has effective axial symmetry, the averaging of cos 2φ causes the second term to go to zero, leading to the simplified form of eq 1.<sup>14</sup> Effective axial symmetry is generally achieved by fast internal rotations or by symmetrical motions about the axis of complexation.

Although a significant contact term contribution is unlikely, in order to use eq 1 as a structural probe it is desirable to determine

(6) R. E. Graves and P. I. Rose, *J. Chem. Soc., Chem. Commun.*, 630 (1973).

(7) Ian M. Walker, L. Rosenthal, and M. S. Quereshi, *Inorg. Chem.*, **10**, 2463 (1971).

(8) R. L. Caret and A. N. Vennos, *J. Org. Chem.*, **45**, 361 (1980).

(9) R. L. Caret, A. N. Vennos, M. Zapf, and J. J. Ubel, *Tetrahedron Lett.*, **22**, 2085 (1981).

(10) J. I. Seeman and J. F. Whidby, *J. Org. Chem.*, **41**, 1585 (1976).

(11) C. S. Springer, Jr., D. W. Meek, and R. W. Sievers, *Inorg. Chem.*, **6**, 1105 (1967).

(12) T. P. Pitner and J. F. Whidby, *Anal. Chem.*, **51**, 2203 (1979).

(13) R. E. Sievers, "NMR Shift Reagents", Academic Press, New York, N.Y., 1973.

(14) Attempts at fitting all of eq 1, including the nonaxial term, resulted in generally poorer fits and in many cases resulted in a nonconvergence of the fitting process.

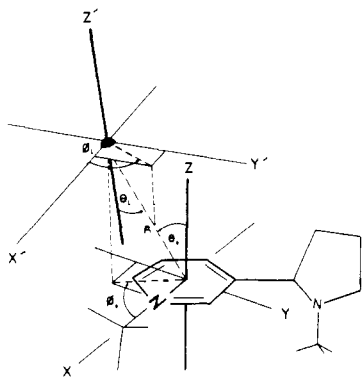


**Figure 1.** Coordinate system for the lanthanide/nicotine *N*-methiodide complex, where  $X'$ ,  $Y'$ ,  $Z'$  are the coordinate axes for the shift reagent.

with some degree of confidence the contribution of the dipolar term. For this reason, the structure-independent method of Reilly and co-workers<sup>15</sup> provides an attractive approach because it does not require definition of the principal magnetic axis of the shift reagent. Rather than assuming a preferred orientation of the complex, this method relies more heavily on the established theoretical shift parameters of Bleaney<sup>16</sup> and Golding<sup>17</sup> for the different lanthanide ions of a particular series. The experimental shifts from a series of lanthanide ions are fit to eq 2, where  $S_{mn}$

$$S_{mn} = F_n \langle S_z^g \rangle_m + G_n C_m + K_n \quad (2)$$

is the observed shift of nucleus,  $n$ , with lanthanide,  $m$ .  $F_n$  and  $G_n$  are the calculated contact and dipolar terms, respectively, which depend on the nucleus observed.  $\langle S_z^g \rangle_m$  and  $C_m$  are the theoretical contact and dipolar parameters for each metal ion.  $K_n$  is the experimental complex formation shift which was determined from  $\text{La}(\text{fod})_3$  complexes and assumed constant over the series of LIS experiments. With use of the shift data from LIS experiments run with five different LSR's, the fitted  $G_n$  and  $F_n$  values for each nucleus in **1** were determined with a standard least-squares program. Table I lists the observed and calculated shifts for each proton in **1** with the corresponding  $G_n$  and  $F_n$  values. For each  $^1\text{H}$  shift observed, the computed  $G_n$  and  $F_n$  values indicated a predominance of dipolar interactions. The standard deviations reported in Table I are a consequence of the least-squares approach to estimating the  $G_n$  and  $F_n$  values. Using a more exact method for calculating  $G_n$  and  $F_n$  for each nucleus would lead to results that qualitatively parallel the conclusions drawn here.

In studies of the solution conformation of substrates where the Ln is visualized as coordinating with a specific donor atom of the substrate, the principal magnetic axis and vector,  $\mathbf{R}$  (see Figure 1), in many cases are assumed coincident. However, use of the shift data alone for this study would require fitting six parameters in order to define the relative positions of the two complexing species. As an alternative to fitting six parameters, the LIS data with  $\text{Yb}(\text{fod})_3$ , known to possess negligible contact contributions, were used in conjunction with relaxation data from  $\text{Gd}(\text{fod})_3$  experiments.

A second important property of the paramagnetic shift reagents, and particularly with  $\text{Gd}(\text{III})$ , is to enhance or replace existing relaxation pathways. Many researchers<sup>18-22</sup> have successfully used spin-lattice relaxation ( $T_1$ ) measurements of nuclei complexed with paramagnetic ions as a tool for quantitating the geometry

(15) C. N. Reilly, B. W. Good, and R. D. Allendoerfer, *Anal. Chem.*, **48**, 1446 (1976).

(16) B. Bleaney, *J. Magn. Reson.*, **8**, 91 (1972).

(17) R. M. Golding and P. Ryykko, *Mol. Phys.*, **26**, 1399 (1973).

(18) G. R. Sullivan, *J. Am. Chem. Soc.*, **98**, 7162 (1976).

(19) B. T. Pennington and J. R. Cavanaugh, *J. Magn. Reson.*, **31**, 11 (1978).

(20) G. A. Elgavish and J. Reuben, *J. Am. Chem. Soc.*, **100**, 3617 (1978).

(21) J. Reuben and J. S. Leigh, *J. Am. Chem. Soc.*, **94**, 2789 (1972).

(22) T. D. Marinetti, G. H. Snyder, and B. D. Sykes, *Biochemistry*, **16**, 647 (1977).

**Table II.** Experimental Proton  $T_1$  Rates<sup>a</sup> and Calculated<sup>b</sup> Relative Distances with  $\text{Gd}(\text{fod})_3$

proton	$1/T_1 \times 10^{-3}$	rel dist
$N'$ - $\text{CH}_3$	$0.17 \pm 0.02$	0.55
$2'$	$0.28 \pm 0.08$	0.59
$5'$	$0.22 \pm 0.02$	0.58
$N$ - $\text{CH}_3$	$2.6 \pm 0.14$	0.86
2	$1.1 \pm 0.08$	0.75
4	$0.65 \pm 0.03$	0.69
5	$2.2 \pm 0.84$	0.84
6	$6.2 \pm 1.00$	1.00

<sup>a</sup> Determined from the slopes of plots of  $T_1$  vs. the molar ratio of  $[\text{Gd}(\text{fod})_3]/[\text{substrate}]$ . <sup>b</sup> Calculated with the  $r^6$  distance relationship.

**Table III.** Absolute  $^1\text{H}$ -Ln Distances Calculated from Equation 3 with  $^1\text{H}$  Relaxation Data

proton	distance, Å	proton	distance, Å
$N'$ - $\text{CH}_3$ <sup>a</sup>	8.2	$N$ - $\text{CH}_3$ <sup>a</sup>	5.2
$2'$	7.6	2	6.0
$5'$	7.9	4	6.6
		5	5.4
		6	4.5

<sup>a</sup> Distances reported for the methyl resonances are an average of the three individual proton distances.

of a substrate molecule. Thus nuclei close to the site of complexation will have shortened  $T_1$  values (i.e., enhanced electron-nuclear relaxation rates). And since the electron-nuclear dipole-dipole relaxation mechanism is suspected to be dominant, a sixth power distance dependency, with no significant angular term, is predicted. This sixth power dependence allows for the simple calculation of the relative nucleus/metal distances, as shown in Table II. The observed  $T_1$  values and subsequent relative distance calculations are in perfect agreement with the LIS results, locating the LRR in the proximity of the pyridyl nitrogen.

When determining the absolute  $^1\text{H}$ /metal distances, an approach similar to that used by Lenkinski et al.<sup>23</sup> was taken which utilizes a modified version of the Solomon-Bloembergen equation.

$$\frac{1}{T_1^{\text{obsd}}} = \frac{2\gamma_H^2\beta^2S(S+1)g^2}{15d^6} \left( \frac{3\tau_c}{1 + \omega_H^2\tau_c^2} + \frac{7\tau_c}{1 + \omega_S^2\tau_c^2} \right) \quad (3)$$

This equation relates the observed relaxation rate,  $1/T_1^{\text{obsd}}$ , using  $\text{Gd}(\text{fod})_3$ , to the distance,  $d$ , between the relaxation reagent and the observed nucleus.  $\omega_H$  and  $\omega_S$  are the proton and electron Larmor frequencies, respectively, and  $\tau_c$  is the correlation time of the complex. It is of interest to note that  $\tau_c$  is composed of three components as seen in eq 4, where  $\tau_s$  is the electron spin

$$\frac{1}{\tau_c} = \frac{1}{\tau_s} + \frac{1}{\tau_r} + \frac{1}{\tau_m} \quad (4)$$

relaxation time of the paramagnetic electrons,  $\tau_r$  is the rotational correlation time of the complex, and  $\tau_m$  is the mean lifetime of the complex. From an analysis of the  $^{13}\text{C}$   $T_1$  values of the conformationally rigid pyridine carbon nuclei with  $\text{La}(\text{fod})_3$ ,  $\tau_r$ , corrected for NOE, was calculated to be  $3.42 \times 10^{-11}$  s.<sup>24</sup> The electron relaxation rate ( $\tau_s$ ) for  $\text{Gd}(\text{III})$  is reported as being greater than  $10^{-9}$  s, especially with the symmetrical fod-type relaxation reagent.<sup>25</sup> For paramagnetic reagent complexes involving rela-

(23) R. E. Lenkinski, private communication.

(24) The value of  $\tau_r$  was calculated from the equation which describes the relaxation rate of a protonated  $^{13}\text{C}$  nucleus by the attached protons

$$T_1^{-1} = N \frac{(\hbar^2\gamma_C^2\gamma_H^2)}{r_{\text{CH}}^6} \tau_r = NK\tau_r$$

where  $r_{\text{CH}}$  is 1.1 Å,  $N$  is the number of attached protons, and  $K$ , a constant, is  $3.56 \times 10^{10}$  s<sup>-2</sup>. D. M. Doddrell, *Pure Appl. Chem.*, **49**, 1385 (1977).

(25) T. D. Marinetti, G. H. Snyder, and B. D. Sykes, *Biochemistry*, **15**, 4600 (1976).

Table IV. Observed and Calculated Shifts for Nicotine *N*-Methiodide/Yb(fod)<sub>3</sub>

nucleus	( $\Delta\delta$ ) obsd shift	fitted <sup>1</sup> H shifts	fitted <sup>13</sup> C shifts	combined fit shifts	angle, $\theta$ , deg
C2	9.7		12.0	12.4	29.6
C4	8.1		7.2	9.0	34.1
C5	12.7		11.7	16.8	25.8
C6	20.9		21.7	29.3	11.6
C2'	5.2		3.4	2.9	43.9
C3'	1.8		2.0	0.58	54.5
C4'	1.5		0.98	-0.26	56.5
C5'	2.3		1.4	0.88	48.7
CH <sub>3</sub> '	2.4		2.2	2.2	35.5
CH <sub>3</sub>	19.2		17.9	19.6	23.5
H2	9.6	10.7		7.6	35.7
H4	7.4	6.9		4.7	40.7
H5	13.4	14.5		12.3	31.3
H6	35.7	35.1		33.6	7.8
H2'	5.0	3.6		1.9	46.7
standard deviation (ppm) $\pm$		1.6	1.4	3.3	
R factor (%)		$\leq 1$	3.9	$\leq 1$	

tively small substrate molecules,  $\tau_m$  is found to be on the order of  $10^{-8}$ – $10^{-7}$  s.<sup>23</sup> Of the three contributing factors,  $\tau_c$  is dominated by  $\tau_r$  and therefore  $\tau_r$  is used to calculate the absolute proton/metal distances as given in Table III. The value of  $\tau_r$  is substituted in eq 3 for the overall correlation time  $\tau_c$ . In the case of the methyl proton distances, the reported values represent an average arising from free rotation of the methyl group. The accuracy associated with the absolute distances is directly dependent upon the uncertainty in the  $T_1$  measurements, determined to be on the order of  $\pm 10$ – $15\%$ .

With LSR's and LRR's supplying independent structural information and assumed to have similar solution geometries with respect to the complexing substrate, it is then possible to use these data as experimental "checks" and also in a complementary fashion to better define the solution geometry.

**Geometry of the Ln/Anion-1 Complex.** The initial set of coordinates for **1** was derived from the molecular coordinates reported for nicotine with the addition of the pyridine *N*-CH<sub>3</sub> group.<sup>26</sup> Experimental observations, namely nuclear Overhauser effect (NOE) measurements and the average proton coupling constants between H<sub>2</sub>'/H<sub>3</sub>'<sub>a,b</sub> of both the complexed and uncomplexed substrate, revealed that the inherent ring-ring configuration and conformation of the pyrrolidine ring are very much like that of nicotine,<sup>27</sup> which supports the use of these coordinates. It would appear that methylation at the pyridine nitrogen to form the methyl iodide salt and subsequent LSR complexation do not distort the overall solution conformation of the substrate when compared to nicotine. When *N*-methylpyridinium iodide was used as a model, coordinates for the pyridyl *N*-methyl group were obtained from an earlier paper of Lalancette et al., which reported the X-ray crystallographic data for that compound.<sup>28</sup>

To first locate the Ln ion, the distances calculated from the  $T_1$  values were fit to the  $r^6$  relationship employing a three-parameter least-squares fit. This fitting procedure minimized the standard deviation between the calculated (from eq 4) distances and fitted distances while systematically varying the position of the Ln ion. The results of this fit produced a computer-refined distance vector, **R**, with coordinate angles  $\theta_s$  and  $\phi_s$ , where **R** is the distance between the Ln ion and the origin of the substrate

(26) T. P. Pitner, W. B. Edwards, III, R. L. Bassfield, and J. F. Whidby, *J. Am. Chem. Soc.*, **100**, 246 (1978).

(27) The average <sup>1</sup>H coupling constant of 7.6 Hz for H2', H3' of **1** compares with  $J(2,3a) = 9.0$  and  $J(2,3b) = 7.8$  Hz of nicotine. NOE experiments, where the H(2) and H(4) protons were saturated, produced enhancement in H(2') of 11% and <5%, respectively. These values suggest not only a perpendicular conformation of the two rings but also that one conformer predominates significantly.

(28) R. A. Lalancette, W. Furey, J. N. Constanza, P. R. Hemmes, and F. Jordan, *Acta. Crystallogr.*, **834**, 2950 (1978).

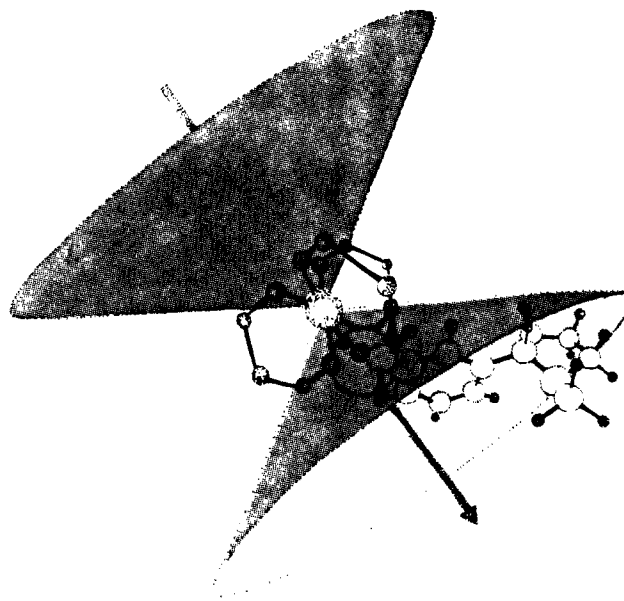


Figure 2. A three-dimensional illustration of the lanthanide complexed ion pair depicted inside the dipolar field shielding boundaries of the shift reagent.

coordinate system. The substrate polar coordinate system is arbitrarily defined with the *X* and *Y* axes lying in the plane of the pyridine ring with the *X* axis projected along the *N*-*C4* axis. The *Z* axis is then perpendicular to the plane of the pyridine ring (see Figure 1).

With the effective spatial position of the metal provided by the relaxation data, a second fit was run to define the orientation of the principal magnetic axis of the metal with respect to the previously described vector, **R**. This fitting procedure was run with Yb(fod)<sub>3</sub> induced <sup>1</sup>H and <sup>13</sup>C shift data along with the previously determined Ln coordinates in order to calculate the best fit values of  $K_1$  (from eq 1),  $\theta_L$ , and  $\phi_L$ . From these overall angles and a knowledge of the substrate conformation, the mean values for  $r_i$  and  $\theta_i$  of eq 1 for each individual nucleus can be calculated. In all the fits done, the coordinates of the substrate were not varied. This in effect assumes a fixed or predominant solution geometry. However, it should be re-emphasized that shift reagent data represent information only on the weighted average Ln/nuclei geometries. Table IV lists the results of the second fit by using the <sup>1</sup>H and <sup>13</sup>C data separately and then combining both data sets.

Agreement between the observed and calculated shifts of the combined fit is quite good considering that ion paired interactions necessarily increase the Ln/nuclei distances. Along with the increased Ln/nuclei distances comes the possibility for increased relative motions of the two interacting species causing a complex averaging of the induced shifts, not accounted for in the fitting procedures. As would be expected, the agreement between calculated and observed shifts is worse for nuclei with  $\theta$  near the "magic angle" ( $54.7^\circ$ ) and having small shifts, since the function  $1 - \cos^2 \theta$  is changing most rapidly at this angle and since the small shift values will be weighted less in the least-squares fit.

The results of fitting the data were not able to provide a statistically significant preference for the two probable interring orientations. However, a second question concerning the position of the Ln ion relative to the pyridine ring was answered by these data by using a distance program that calculates the distance between any two atoms in a molecule where the molecular coordinates are known. Lanthanide to nucleus distances were calculated for each of the two possibilities. A correlation was obtained only when the Ln was positioned on the opposite side of the pyridine ring relative to the pyrrolidine *N*-CH<sub>3</sub> group. Distances calculated for the syn (same side of pyridine ring as pyrrolidine *N*-CH<sub>3</sub>) configuration were too small to correlate with either the relaxation or induced shift data observed. It stands to reason that if the two rings are taken to be perpendicular, steric

hinderance caused by the pyrrolidine  $N\text{-CH}_3$  would cause the LSR/ $I^-$  moiety to migrate to the back side of the pyridine ring.

Rotation of the Ln ion results in the motionally averaged orientation of the complex depicted in Figure 2 which is fixed within the statistical uncertainty of  $\pm 5.7^\circ$  for angles  $\theta_L$  and  $\phi_S$ .

The association is visualized as an interaction between the LSR and the anion (iodide) which results in the paramagnetic effect experienced by nuclei of the cation or substrate. It would appear that the association is such that the overall net charge of the LSR/anion moiety remains negative and that the initial charge affinity of the anion is not greatly changed, as evident by the calculated lanthanide position. When the X-ray data reported for  $N$ -methylpyridinium iodide are used as a model, the closest approach of the iodide to the pyridine ring was reported as 3.76 Å from the nitrogen and 3.73 Å above the plane of the ring. The results from this study position the Ln ion approximately 3.87 Å above the C(6)-H(6) bond (or the plane of the pyridine ring). Although there is no direct evidence presented here supporting the actual position of the iodide, when viewing molecular models it is not unreasonable to depict the iodide as being sandwiched in between the LSR and the cation in a linear fashion as shown in Figure 2. The usual, directly coordinated, Ln distances derived from LSR interactions are reported as approximately 2.5-2.65 Å. Significantly larger distances are observed with ion pair complexes of LSR's.

## Conclusion

The use of LSR's and LRR's as tools for quantitating the time-averaged solution geometry of an organic salt proves to be a workable technique. The results of this study show that LIS and relaxation data, taken separately or combined, yield structural information comparable to data obtained from studies of directly coordinated Ln complexes. Calculations of this type rarely produce a single point that will exactly define the time-averaged position of the lanthanide ion; however, the fits obtained from the present data strongly suggest that the probability of such a point is not an incorrect approximation. Ion pair complexes of this type result in induced shifts that are primarily dipolar in origin with no significant contact contribution. Consequently, the information obtained from distance and angle calculations serves to define the position of the anion in solution or to quantitate the solution geometry of the cation.

**Acknowledgment.** The author wishes to acknowledge the contribution of Drs. T. Phil Pitner, J. F. Whidby, and J. I. Seeman. He also wishes to thank Dr. R. E. Lenkinski and the late Dr. C. N. Reilley for useful discussions and Anne Donathan for secretarial assistance.

**Registry No.** 1, 21446-46-8; Er(fod)<sub>3</sub>, 17978-75-5; Eu(fod)<sub>3</sub>, 17631-68-4; Ho(fod)<sub>3</sub>, 18323-97-2; Pr(fod)<sub>3</sub>, 17978-77-7; Yb(fod)<sub>3</sub>, 18323-96-1; Gd(fod)<sub>3</sub>, 18323-96-1.

## Lanthanide Induced Shift and Relaxation Rate Studies of Aqueous L-Proline Solutions

Mangal Singh,<sup>†</sup> Joe J. Reynolds, and A. Dean Sherry\*

Contribution from the Department of Chemistry, University of Texas at Dallas, Richardson, Texas 75080. Received September 2, 1982

**Abstract:** The structure of aqueous L-proline at pH 3 has been studied with use of the lanthanide-induced-shift technique. Paramagnetic nuclear shifts and enhancement of nuclear-relaxation rates have been measured for all  $^{13}\text{C}$  and  $^1\text{H}$  nuclei of L-proline in the presence of ten different lanthanide cations. The relaxation-rate data indicate that isostructural complexes are formed between proline and all ten lanthanide cations. An attempted separation of the observed lanthanide-induced shifts into pseudocontact and contact components with use of the Reilley method (C. N. Reilley, B. W. Good, and R. D. Allendoerfer, *Anal. Chem.*, **48**, 1446 (1976)) gave inconsistent results for the  $\alpha$  and carboxyl carbons indicating that either the shifts at these nuclei have a nonaxial dipolar contribution or the hyperfine coupling constant is lanthanide ion dependent. The pseudocontact shifts at  $C_\beta$ ,  $C_\gamma$ , and  $C_\delta$  and at all protons conform well to the axial symmetry model with the lanthanide ion principal symmetry axis intersecting a single oxygen atom  $2.9 \pm 0.1$  Å from the lanthanide cation.

The trivalent lanthanide cations have found widespread use as NMR shift and relaxation probes of the dynamic solution conformations of molecules.<sup>1</sup> The shift method relies upon the measurement of paramagnetic shifts in several nuclei of a molecule, a purification of each measured LIS of any contact-shift contribution, and a comparison of the resulting pseudocontact shifts with those calculated from an appropriate dipolar model which contains both distance and angular parameters. The interpretation of relaxation data to obtain relative  $\text{Ln}^{3+}$ -nuclei distances is more direct but requires the assumption of an identical correlation time for all nuclei in the molecule. Recent LIS studies on some simple carboxylates<sup>2,3</sup> and amino acids<sup>3,4</sup> have suggested that these ligands do not form isostructural complexes with all lanthanide cations. Elgavish and Reuben have used relaxation data to show that sarcosine forms isostructural complexes with all lanthanide cations<sup>5</sup> and proposed<sup>6</sup> that the earlier  $\text{Ln}^{3+}$ -ligand structural changes resulted from a choice of improper models for the interpretation

of LIS data. In this paper, we report lanthanide-induced shifts and relaxation rates for all  $^{13}\text{C}$  and  $^1\text{H}$  nuclei in the complexes of L-proline with ten different paramagnetic cations. The relaxation data show that isostructural complexes are formed with all ten lanthanide cations. The pseudocontact LIS data for all nuclei except the carboxyl and  $\alpha$  carbons conform nicely to the effective axial symmetry dipolar model while the aforementioned carbon shifts contain an additional contribution which could lead to incorrect conclusions about structural alterations along the  $\text{Ln}^{3+}$  series.

(1) C. M. Dobson and B. A. Levine, "New Techniques in Biophysics and Cell Biology", Vol. 3, Wiley, New York, 1976, Chapter 2.

(2) B. A. Levine, J. M. Thornton, and R. J. P. Williams, *J. Chem. Soc., Chem. Commun.*, 669 (1974).

(3) B. A. Levine and R. J. P. Williams, *Proc. R. Soc. London, Ser. A*, **345**, 5 (1975).

(4) A. D. Sherry and E. Pascual, *J. Am. Chem. Soc.*, **99**, 5871 (1977).

(5) G. A. Elgavish and J. Reuben, *J. Am. Chem. Soc.*, **100**, 3617 (1978).

(6) J. Reuben and G. A. Elgavish, *J. Magn. Reson.*, **39**, 421 (1980).

<sup>†</sup> On study leave from Guru Nanak Dev University, Amritsar, India.